Journal of Structural Geology, Vol. 9, No. 7, pp. 819 to 833, 1987
Printed in Great Britain

0191-8141/87 $03.00 + 0.00
Pergamon Journals Ltd.

Heterogeneous deformation and quartz crystallographic fabric transitions: natural examples from the Moine Thrust zone at the Stack of Glencoul, northern Assynt

R. D. LAW

Department of Earth Sciences, The University, Leeds LS2 9JT, U.K.

(*Received* 20 *August* 1986; *accepted in revised form* 2 *December*)

Abstract—Quartz crystallographic fabric transitions in well-exposed mylonites immediately beneath the Moine Thrust at the Stack of Glencoul (NW Scotland) have been investigated by optical microscopy, X-ray texture goniometry and Orientation Distribution Function analysis. A progressive change is observed from asymmetrical kinked single girdle c-axis fabrics at 0.5 cm beneath the Moine Thrust, through asymmetrical Type I cross-girdle fabrics to symmetrical Type I cross-girdle fabrics at 30 cm beneath the thrust. This c-axis fabric transition is accompanied by a transition from asymmetrical single a-axis maximum fabrics (0.5 cm beneath the thrust) through asymmetrical two maxima fabrics to essentially symmetrical two maxima a-axis fabrics. ODF analysis of these $S > L$ and $L - S$ tectonites indicates that c-axis positions on the 'leading edge' of the fabric skeleton are related by a common ⟨a⟩ direction oriented within the XZ plane at a moderate angle to the lineation (X). In contrast, c-axis positions on the peripheral 'trailing edge' are related by a positive (r) rhomb pole oriented close to Z; ⟨a⟩ directions lying within this common rhomb plane progressively change through 180° in orientation traced around the c-axis fabric skeleton. Such contrasting 'single crystal' rhomb ⟨a⟩ preferred orientations on the 'leading' and 'trailing' edges of the fabric skeleton are interpreted as indicating localized (grain scale) plane strain and flattening deformation, respectively. They result in tectonites with essentially symmetrical c- and a-axis fabrics which display strongly asymmetrical positive (r) and negative (z) rhomb pole figures. The observed transition in quartz c- and a-axis fabrics is interpreted as indicating an increasing importance of non-coaxial plane-strain deformation as the Moine Thrust is approached. Even immediately (<1 cm) beneath the thrust, however, flow has still significantly departed from bulk simple shear and involved an important (heterogeneous) component of contemporaneous flattening deformation.

INTRODUCTION

CRYSTALLOGRAPHIC fabrics are commonly used as a research tool for studying the conditions and processes of deformation associated with the intracrystalline flow of rocks. Theoretical studies (e.g. Lister *et al.* 1978) indicate that the development of crystallographic fabrics in quartzites during plastic deformation is governed by three main factors: (1) the strain path or kinematic framework; (2) the magnitude and symmetry of strain; and (3) the particular combination of crystallographic glide systems operative during deformation.

The interpretation of such fabrics is based upon a series of generally accepted assumptions. One of the most important assumptions is that the symmetry of deformation (i.e. the strain path) will be reflected in the symmetry of the resultant fabric (see Lister & Williams 1979 for review). Thus, fabrics which are symmetrical with respect to foliation and lineation have been interpreted as indicating essentially coaxial strain paths, and asymmetrical fabrics indicative of non-coaxial flow. Such kinematic interpretations are supported by the theoretical studies of Lister and co-workers (e.g. Lister & Hobbs 1980).

Most geological structures owe their development to heterogeneous flow (see review by Lister & Williams 1983). Thus, if crystallographic fabrics do accurately reflect the local strain path, then the study of the spatial distribution of fabric symmetry within such structures may be a powerful key to understanding the flow patterns (strain paths) associated with formation of these structures.

For example, in a recent publication (Law *et al.* 1984) on the Eriboll region of the Moine Thrust zone, petrofabric evidence was presented for strain path partitioning within the mylonitic Cambrian quartzites of the Upper Arnaboll thrust sheet. This optical study of quartz c-axis preferred orientation, which was supported by microstructural studies, indicated that whilst the internal regions of the thrust sheet (located immediately beneath the Moine Thrust) were deformed under dominantly coaxial strain paths, deformation near the margins of the sheet was strongly non-coaxial. Due to lack of suitable outcrops, however, the transition zone between these inferred kinematic domains could not be accurately located, and the detailed nature of the crystallographic fabric transition between these domains remained unknown.

Thirty km to the south of Loch Eriboll, at the Stack of Glencoul (Grid Ref. NC 28882876), in the northern part of the Assynt region, the contact between the Moine Thrust and the underlying sheet of mylonitic Cambrian quartzites is well exposed, facilitating a detailed study of the relationships between crystallographic preferred orientation, microstructure and proximity to the thrust surface. Foliation (XY) within these mylonites is oriented parallel to the thrust surface and contains a grain shape lineation which plunges at 18°/118°, subparallel to the Moine Thrust zone transport direction. Mylonites from the Stack of Glencoul range from $S > L$

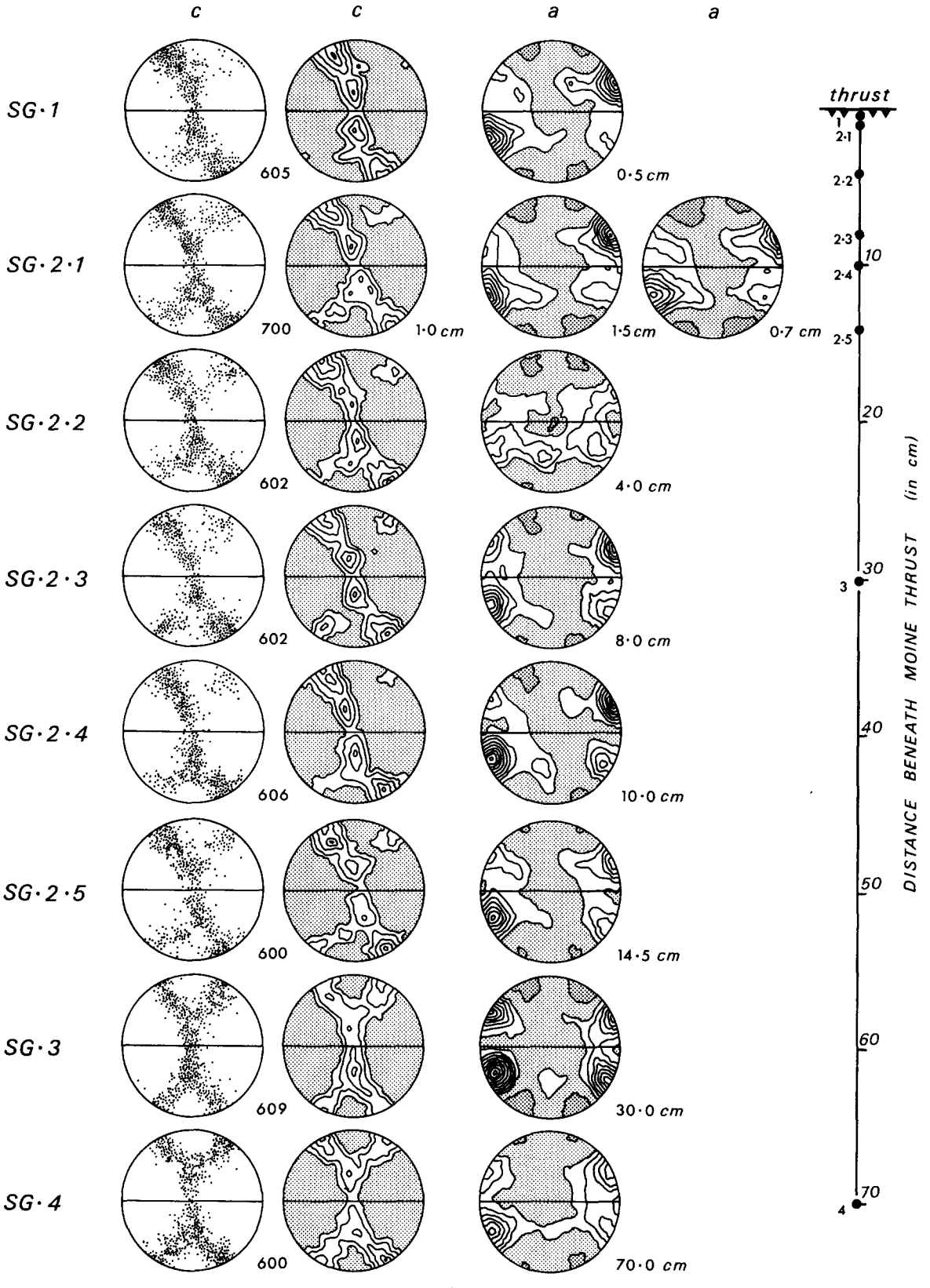

Fig. 1. Transition in quartz c- and a-axis fabrics with increasing distance beneath the Moine Thrust at the Stack of Glencoul. Specimen numbers indicated in left-hand column, and dots on the right-hand section. Contour intervals of optically measured c-axis fabrics—1, 2, 3, 4, 5 and 6 times uniform distribution; less than 1.0 times uniform distribution stippled. Contour intervals of a-axis fabrics 0.5, 1.0, 1.25, 1.5, 1.75, . . . 3.0, 3.25 times uniform distribution; less than 0.5 and 0.5–1.0 times uniform distribution, heavy and light stipple, respectively. Fabrics contoured using a modified version of the computer program described by Starkey (1970). All lower hemisphere equal-area projections viewed towards the NNE. For details of specimen locations see Law *et al.* (1986, fig. 2).

to $L - S$ tectonites and locally display pinch and swell structures on surfaces oriented both parallel (XZ) and perpendicular (YZ) to the lineation. Variation in c-axis fabrics and microstructures within those tectonites located immediately (<70 cm) beneath the Moine Thrust have previously been described by Law *et al.* (1986, fig. 7).

In this paper these optically measured c-axis fabrics are compared (Fig. 1) with previously unpublished a-axis fabric data obtained from the same specimens by X-ray texture goniometry at ETH, Zurich. Details of the detected variation in quartz c- and a-axis fabrics with distance beneath the Moine Thrust will be described, and possible reasons for the fabric variations (transitions) discussed.

Generally this type of petrofabric analysis assumes that at the scale of observation (i.e. the thin-section scale) deformation is homogeneous. This assumption, which is a basic element of the fabric simulation studies of Lister and co-workers (e.g. Lister *et al.* 1978), requires that each grain within an aggregate undergoes the same shape change as the bulk specimen. Such an assumption (which is commonly made in petrofabric analyses) may not be universally applicable. For example, in the experimental intracrystalline deformation of calcite polycrystals, Van Houtte *et al.* (1984) and Wenk *et al.* (1986) demonstrated that the strain path followed by individual grains may significantly depart from the strain path imposed upon the bulk specimen. In this paper the possibility of such heterogeneous (grain scale) deformation is investigated within representative specimens through the study of Orientation Distribution Functions (ODFs) calculated from X-ray derived pole figure data.

Located immediately beneath the Moine Thrust, specimens SG·1 and SG·2 are completely recrystallized tectonites (Type II $S - C$ mylonites of Lister & Snoke 1984) which, in XZ sections, display (Law *et al.* 1986, figs. 4g & h) a preferred alignment (S_B) of dynamically recrystallized quartz grains which is oblique to the mylonitic foliation (S_A). The sense of obliquity between S_A and S_B is consistent with non-coaxial deformation associated with WNW directed overthrusting. Such microstructural shear-sense indicators have not been observed within the less intensely deformed and recrystallized quartzites (e.g. specimens SG·3 and SG·4 in Fig. 1) located at greater distances beneath the thrust plane. Location details for both these specimens (SG·1–SG·4) situated at less than 0.7 m beneath the thrust, and other specimens (SG·5–SG·13) situated at greater distances beneath the thrust, may be found in Law *et al.* (1986, fig. 2).

The crystallographic fabric data are displayed on equal area, lower hemisphere spherical projections whose plane of projection contains the specimen lineation (X) and pole to foliation (Z); in all these projections foliation is vertical, and lineation within the foliation horizontal. In geographical terms all these projections are viewed towards the NNE, the lineation being represented as a horizontal structure.

QUARTZ CRYSTALLOGRAPHIC FABRICS

Quartz c-axis fabrics

All specimens collected from immediately beneath the Moine Thrust at the Stack of Glencoul yield strongly defined c-axis fabrics (Fig. 1) whose density distributions about the skeletal outline (Lister & Williams 1979) appear to vary in a systematic fashion with distance beneath the thrust plane. Details of these c-axis fabric skeletons are presented in Table 1 for individual specimens.

At a distance of 0.5 cm beneath the thrust plane, the c-axis fabric of specimen SG·1 consists of a kinked single-girdle oriented oblique to the mylonitic foliation (S_A), and containing the inferred Y direction (Fig. 1). Detailed optical study of this totally recrystallized tectonite (grain size 5–10 μm) indicates, however, that there are some grains whose c-axes do not belong to this single-girdle population; these grains have their c-axes positioned on a complementary, but much more weakly defined, cross-girdle limb (Fig. 1).

Specimen SG·2 consists of five quartzite layers (SG·2·1–SG·2·5) separated by phyllosilicate-rich horizons (Law *et al.* 1986, fig. 3d). Optically measured c-axes from these layers of recrystallized quartz define unequally populated Type I (Lister 1977) cross-girdle fabrics (Fig. 1).

The c-axis fabrics from specimens SG·1 and SG·2 are strongly asymmetrical with respect to foliation and lineation, both in terms of skeletal outline (topology) and density distribution. A consistent sense of asymmetry is displayed in each specimen (Fig. 1).

The degree of external fabric asymmetry (Platt & Behrmann 1986, p. 30) may be expressed by: (1) the obliquity, measured in the XZ plane, between the pole to foliation (Z) and the 'leading' (ESE dipping) and 'trailing' (WNW dipping) peripheral legs of the fabric skeleton (c_1 and c_2, respectively, in Table 1); and (2) the obliquity of the central girdle segment with respect to the foliation trace (defined by ψ in Table 1). Inspection of Table 1 indicates the consistent nature of both the sense and degree of external skeletal c-axis fabric asymmetry for specimens SG·1 and SG·2. The degree of internal fabric asymmetry may be defined by the relative inclination of the 'leading' and 'trailing' peripheral legs with respect to the central girdle segment (ω_1 and ω_2, respectively, in Table 1). From inspection of Table 1 it is clear that the 'leading edge' of the fabric skeleton in specimens SG·1 and SG·2 has far less of a kinked pattern (small ω_1 values) than the corresponding 'trailing edge' (larger ω_2 values).

Within specimens SG·3 and SG·4, however, the degree of both internal and external c-axis skeletal fabric asymmetry is considerably reduced. These Type I (Lister 1977) cross-girdle c-axis fabrics were measured on relict old grains set in a matrix of dynamically recrystallized quartz (50% recrystallization by volume fraction). For both specimens the central girdle segment of the cross-girdle fabric is oriented sub-perpendicular to the folia-

Table 1. Details of c- and a-axis fabric symmetry for specimens SG·1–SG·4 (c.f. Fig. 1). External skeletal fabric symmetry is characterized by c_1, c_2, ψ and a_1, a_2. Internal fabric symmetry characterized by ω_1 and ω_2. Ma_1 and Ma_2—maximum a-axis density on the WNW and ESE plunging a-axis maxima lying within the XZ plane. Distances (d) of individual specimens beneath the Moine Thrust indicated

specimen	ψ	c_1	c_2	a_1	a_2	Ma_1 (times	Ma_2 uniform)	ω_1	ω_2	d (in cm)
SG·1	83°	22°	32°	25°	30°	3·0	1·3	26°	60°	0·5
SG·2·1	72°	27°	35°	24°	28°	2·7	1·5	10°	55°	0·7
				27°	25°	3·1	1·5			1·0
										1·5
SG·2·2	82°	30°	40°	29°	30°	1·5	1·5	28°	55°	4·0
SG·2·3	84°	30°	33°	24°	30°	2·7	1·9	26°	55°	8·0
SG·2·4	78°	27°	35°	25°	29°	3·2	1·8	25°	62°	10·0
SG·2·5	74°	27°	35°	24°	30°	2·6	1·7	22°	70°	14·5
SG·3	87°	25°	25°	24°	30°	3·2	2·5	35°	40°	30·0
SG·4	85°	26°	30°	27°	28°	2·4	1·6	38°	55°	70·0

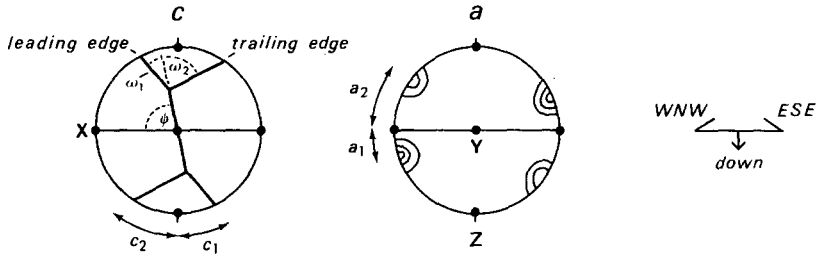

tion (XY), whilst the peripheral legs are similarly inclined to the foliation pole (Z). A much lower degree of internal fabric asymmetry is also indicated within these specimens by the closer ω_1 and ω_2 values (within 5 and 17° of each other in SG·3 and SG·4, respectively). These small internal fabric asymmetries may be compared with the larger differences (Table 1) between ω_1 and ω_2 (27–50°) in specimens SG·1 and SG·2, located at <14.5 cm beneath the Moine Thrust, and the similar small differences (generally 1–5°) between ω_1 and ω_2 (Table 2) within specimens SG·6–SG·13, located at 1.9–8.5 m beneath the thrust (Law *et al.* 1986).

Quartz a-axis fabrics

All specimens are characterized by a-axis fabrics consisting of two maxima aligned within the XZ plane (Fig. 1). In all cases the dominant maximum (Ma_1 in Table 1) plunges to the WNW and the subordinate maximum (Ma_2) plunges ESE. In general the ESE plunging maximum becomes more intense traced away from the thrust surface, resulting in a reduction in the intensity difference between the two maxima.

For example, the scanning area of specimen SG·1, located 0.5 cm beneath the thrust surface, essentially

Table 2. Details of c- and a-axis fabric symmetry within specimens SG·6–SG·13 described by Law *et al.* (1986, figs. 5 and 6) from the Stack of Glencoul. See Table 1 for explanation of parameters used

specimen	ψ	c_1	c_2	a_1	a_2	Ma_1 (times	Ma_2 uniform)	ω_1	ω_2	d (in m)
SG·6	90°	28°	28°	18°	27°	2·0	1·5	53°	50°	1·9
SG·7	90°	25°	27°	22°	25°	2·0	2·0	50°	48°	2·5
SG·8	90°	27°	27°	24°	25°	2·0	2·0	45°	48°	2·9
SG·9	90°	26°	30°					46°	47°	3·55
SG·10	89°	23°	30°	17°	20°	2·5	2·0	43°	53°	4·6
SG·11	87°	27°	26°	18°	21°	4·5	2·0	51°	56°	4·6
SG·12	88°	37°	35°					45°	43°	7·3
SG·13	87°	24°	25°	27°	22°	7·0	3·5	52°	53°	8·5

yields a single intense a-axis maximum occupying the pole position to the corresponding c-axis single-girdle fabric (Fig. 1). This dominant a-axis maximum (3.0-times uniform intensity) is accompanied (Table 1) by a much weaker subsidiary maximum (1.3-times uniform intensity). Within specimen SG·2·1 the ESE plunging a-axis maximum is slightly more clearly developed at 0.7 cm beneath the thrust. The reproducibility of this a-axis fabric has been confirmed by scanning an area at 1.5 cm beneath the thrust in the quartzite layer of specimen SG·2·1 (Fig. 1). In contrast, within specimen SG·3, located at 30 cm beneath the thrust, the ESE plunging a-axis maximum is now more strongly developed (2.5-times uniform) and is of a similar intensity to that of the corresponding WNW plunging principal maximum (3.2 times uniform).

The degree of external a-axis fabric asymmetry may be expressed by the relative inclination to the lineation (X) of the two maxima aligned within the XZ plane. In general the dominant WNW plunging a-axis maximum is inclined at a slightly lower angle (a_1 in Table 1) to the lineation than the subsidiary ESE plunging maximum (a_2). No convincing correlation, however, has been established (Tables 1 and 2) between the difference ($a_2 - a_1$) in a-axis maxima inclination (1–6°) to the lineation and distance beneath the thrust surface.

All quartz mylonites from the Stack of Glencoul are characterized by a-axis maxima which (to a greater or lesser extent) are connected by a broad, weakly populated band of a-axes, defining a small-circle distribution of large opening angle centred about the pole to foliation (Z). This small-circle distribution of a-axes is generally only weakly developed at distances of less than 0.7 m beneath the Moine Thrust (Fig. 1) but is more strongly developed (specimens SG·6–SG·13) at greater distances beneath the thrust (Law *et al.* 1986, fig. 6). Within other geological terrains similar small-circle girdle a-axis fabrics have been exclusively described from S tectonites (Schmid & Casey 1986, Law 1986).

Nature of crystallographic fabric transition

The integration of optical and X-ray texture goniometry studies on quartz mylonites located immediately beneath the Moine Thrust has led to a clear correlation between the pattern of quartz c- and a-axis preferred orientation and distance beneath the thrust surface. This spatial fabric transition consists of a progressive change from asymmetrical dominantly kinked single-girdle c-axis fabrics (0.5 cm beneath the thrust), through Type I (Lister 1977) cross-girdle c-axis fabrics which are asymmetrical with respect to specimen co-ordinates both in terms of skeletal outline and density distribution, to approximately symmetrical Type I cross-girdle c-axis fabrics at 30 cm beneath the thrust (Fig. 1). This transition is accompanied by a clear crystallographically related transition from dominantly single maximum a-axis fabrics (0.5 cm beneath thrust), through two maxima a-axis fabrics which are strongly asymmetrical in terms of density distribution (internal symmetry) and, to a lesser extent, orientation with respect to specimen co-ordinates (external symmetry), to two maxima a-axis fabrics which display a lower density difference between the two maxima (Fig. 1).

Traced away from the thrust surface, this spatial fabric transition essentially involves the progressive development of the 'trailing' (WNW dipping) peripheral leg of the crossed-girdle c-axis fabric accompanied by the strengthening of the subsidiary, ESE plunging, a-axis maximum. This transition is accompanied by a general increase in the degree of internal skeletal c-axis fabric symmetry and, possibly a smaller, less clearly defined, increase in external fabric symmetry. This increased symmetry is most clearly marked at distances of greater than 30 cm beneath the thrust surface (specimens SG·3 and SG·4). A similar high degree of both internal and external symmetry is also displayed (Law *et al.* 1986, figs. 5 and 6) by c- and a-axis fabrics within quartz mylonites located at greater distances beneath the Moine Thrust at the Stack of Glencoul (Table 2).

Kinematic interpretation of crystallographic fabric symmetry

Located close to the Moine Thrust, c- and a-axis fabrics from specimens SG·1 and SG·2 are strongly asymmetrical with respect to foliation and lineation, both in terms of intensity distribution and, to a lesser extent, skeletal outline (Fig. 1). The sense of c- and a-axis fabric asymmetry (see reviews by Bouchez *et al.* 1979, Lister & Williams 1979, Behrmann & Platt 1982, Simpson & Schmid 1983) is consistent with non-coaxial deformation associated with WNW directed overthrusting (sinistral shear sense in Fig. 1). This inferred shear sense is in agreement with that indicated by both the microstructures in these specimens (Law *et al.* 1986, fig. 4h) and also local thrust geometries (see Law *et al.* 1986 for references).

In contrast, at greater distances beneath the Moine Thrust, quartz c- and a-axis fabrics (specimens SG·3 and SG·4) are, particularly in terms of skeletal outline (Table 1), essentially symmetrical with respect to foliation and lineation (Fig. 1) indicating coaxial strain paths. Approximately coaxial strain paths are also indicated by the essentially symmetrical c- and a-axis fabrics (Law *et al.* 1986, figs. 5 and 6) within specimens SG·6–SG·13 (Table 2) located at distances of between 1·9 and 8·5 m beneath the thrust. No convincing microstructural shear sense indicators have been observed in these specimens.

Symmetrical cross-girdle c-axis fabrics have previously been described from the Stack of Glencoul by Christie (1963). These symmetrical fabrics, which were measured on large relict quartz grains, have been contrasted by Riekels & Baker (1977, p. 8) with the corresponding asymmetrical c-axis fabrics calculated from Orientation Distribution Functions (ODFs) obtained through X-ray texture goniometry work on the same specimens. They attribute this discrepancy to the difficulty of measuring c-axes of very small grains (which

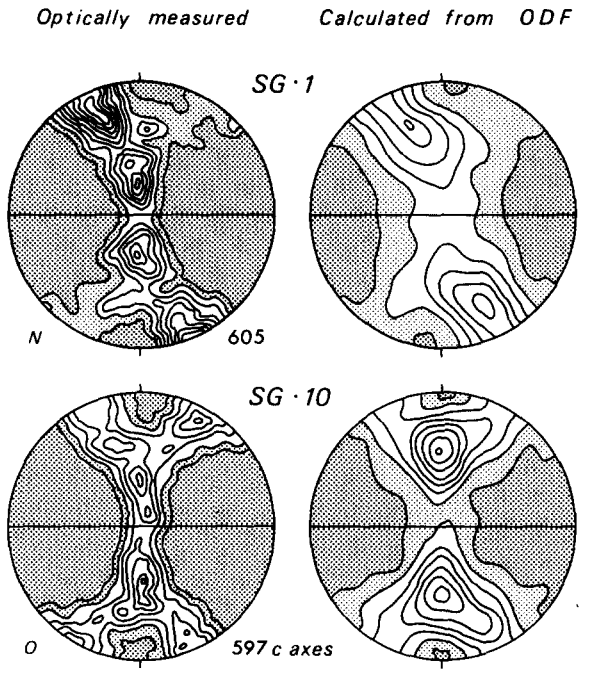

Fig. 2. Comparison of optically measured and calculated c-axis fabrics from specimens SG·1 and SG·10 (scanning areas 0.5 cm and 4.6 m, respectively, beneath the Moine Thrust at the Stack of Glencoul). Specimen SG·1—c-axes optically measured on new grains (N)—100% recrystallization. Specimen SG·10—c-axes optically measured on relic grains (O)—approximately 50% recrystallization. Contour intervals of optically measured fabrics—0.5, 1.0, 2.0, 3.0, . . . 8.0, 9.0 times uniform distribution. Contour intervals of fabrics calculated from ODFs—0.5, 1.0, 1.5, 2.0, . . . 3.5, 4.0 times uniform distribution. For both measured and calculated fabrics, less than 0.5 and 0.5–1.0 times uniform distribution are indicated by heavy and light stipple, respectively. All lower hemisphere equal-area projections viewed towards the NNE. For specimen locations see Law *et al.* (1986, fig. 2).

may form the asymmetrical element of a fabric pattern) with the optical microscope.

ODFs of selected quartz mylonites from the Stack of Glencoul and other areas within the Moine Thrust zone have been calculated at ETH, Zurich, and will form the subject of a separate paper. This study has indicated that there is no significant difference in skeletal symmetry between optically measured and calculated c-axis fabrics, although some differences in density distribution are detected. For example specimen SG·10 (approximately 50% recrystallization to 20 μm grain size) located 4.6 m beneath the Moine Thrust at the Stack of Glencoul, has yielded measured and calculated c-axis fabrics which are almost perfectly symmetrical (both in terms of skeletal outline and intensity distribution) with respect to foliation and lineation (Fig. 2, Table 3). Similarly no significant difference in skeletal symmetry between measured and calculated c-axis fabrics has been detected (Fig. 2, Table 3) within specimen SG·1 (complete recrystallization to 5–10 μm grain size) located at 0.5 cm beneath the thrust.

It should be noted, however, that the density distribution within the calculated c-axis pole figure for specimen SG·10 is intermediate between a cross-girdle and small-circle fabric (Fig. 2) indicating (Marjoribanks 1976, Lister *et al.* 1978, Price 1985, Law 1986) deformation within the flattening field ($1 > K > 0$) of the strain plot. In contrast, optically measured c-axes from this specimen define (both in terms of skeletal outline and density distribution) a cross-girdle fabric (Fig. 2) indicating approximate plane-strain deformation. The former interpretation is more in accord with the oblate grain shape fabric (Schmid & Casey 1986, fig. 2i—specimen RL8330) and small-circle a-axis fabric (Fig. 3) recorded in this tectonite.

Within specimen SG·1 the asymmetrical nature of both the measured and calculated c- and a-axis fabrics (Figs. 1 and 2; Tables 1 and 3) is also reflected in the corresponding m, r and z pole figures calculated from the ODF for this specimen (Fig. 3). Similarly, the symmetrical nature of both the measured and calculated c- and a-axis fabrics (Fig. 2, Table 2) in specimen SG·10 is also reflected in the corresponding calculated m pole figure (Figure 3). Calculation of the corresponding r and z pole figures from the ODF for specimen SG·10, however, has produced totally unexpected fabrics which are strongly asymmetrical with respect to foliation and lineation. Thus although the c, a and m pole figures for specimen SG·10 are symmetrical, the total crystallographic fabric within this tectonite is asymmetrical.

These calculated symmetrical and asymmetrical pole figures for specimen SG·10 must bring into question the general validity of using fabric symmetry in terms of pole figures for c- and a-axes as a kinematic (strain path) indicator.

Table 3. Comparison of symmetry within measured and corresponding calculated c- and a-axis fabrics for specimens SG·1 and SG·10. See Table 1 for explanation of parameters used

specimen	method	ψ	c_1	c_2	a_1	a_2	Ma_1 (times	Ma_2 uniform)	ω_1	ω_2
SG·1	measured	83°	22°	32°	25°	30°	3·0	1·3	26°	60°
SG·1	calculated	85°	24°	32°	23°	32°	3·0	1·2	30°	53°
SG·10	measured	89°	23°	30°	17°	20°	2·5	2·0	43°	53°
SG·10	calculated	92°	25°	25°	19°	21°	2·0	2·0	49°	54°

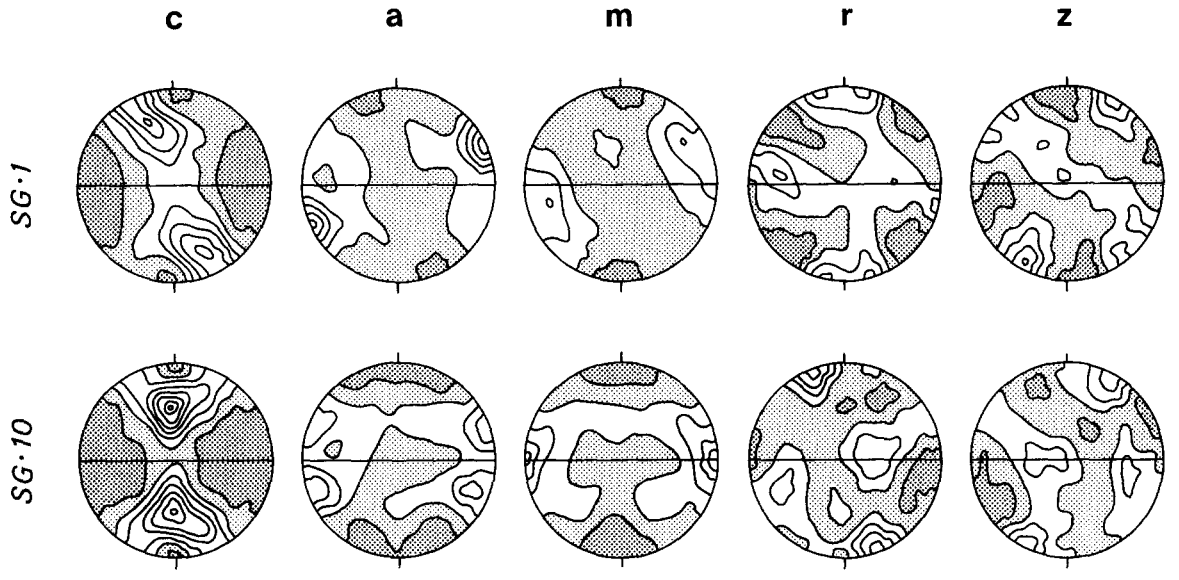

Fig. 3. Crystallographic fabrics (c-, a-, m-, r- and z-axes) calculated from the ODFs for specimens SG·1 and SG·10. Contour intervals—0.5, 1.0, 1.5, 2.0, . . . 3.5, 4.0 times uniform distribution; less than 0.5 and 0.5–1.0 times uniform distribution, heavy and light stipple, respectively. All lower hemisphere equal-area projections viewed towards the NNE.

INDIVIDUAL 'CRYSTAL' PREFERRED ORIENTATION

In order to obtain a more detailed understanding of the relationships between the symmetrical (c, a and m) and asymmetrical (r and z) fabrics within specimen SG·10, an analysis has been made of the most probable (favoured) orientations of poles to second $(11\bar{2}0)$ and first $(10\bar{1}0)$ order prisms (⟨a⟩ and ⟨m⟩ directions, respectively) and positive $(10\bar{1}1)$ and negative $(01\bar{1}1)$ rhombs (r and z, respectively) for individual positions on the c-axis fabric skeleton. Results of this analysis will then be compared with a similar analysis of specimen SG·1.

Details of the techniques involved in these analyses, which involved using data from the ODFs for specimens SG·10 and SG·1, may be found in Schmid *et al.* (1981).

Basal (0001) ⟨*a*⟩ *orientations*

Study of the ODF for specimen SG·10 indicates that grains occupying different positions on the 'leading edge' of the c-axis fabric skeleton (positions 1–18) are related by a common ⟨a⟩ direction (Fig. 4) which is aligned parallel to the WNW plunging maximum in the a-axis pole figure (Fig. 3). The two other ⟨a⟩ directions from the 'leading edge' of the fabric skeleton plot on two small-circle girdles centred about this WNW plunging a-axis maximum (Fig. 4). A similar preferred orientation of 'leading edge' basal ⟨a⟩ systems is displayed by specimen SG·1 (Fig. 4). This high degree of alignment of ⟨a⟩ directions on the 'leading edges' of specimens SG·10 and SG·1 suggests that although the relative activity of different slip planes may vary from grain to grain, the ⟨a⟩ slip direction contained within these planes remains in a constant orientation relative to specimen co-ordinates.

In contrast, on the peripheral 'trailing edge' of the c-axis fabric skeletons (positions 19–29 in SG·1, positions 19–28 in SG.10) the ⟨a⟩ directions define a more streaked out pattern than that observed on the 'leading edge' (Fig. 4). It is this geometrical arrangement of ⟨a⟩ directions corresponding to c-axis positions on the 'trailing edge' of the fabric skeletons which has produced the small circle girdle distribution element in the a-axis pole figures (Fig. 3).

For specimen SG.10, c-axis positions (7–13) on the central segment of the fabric skeleton close to *Y* are characterized by basal planes containing ⟨a⟩ directions aligned parallel to both the WNW and ESE plunging a-axis maxima (c.f. Figs. 3 and 4). A similar alignment of ⟨a⟩ directions is detected on the central segment (positions 7–14) of the fabric skeleton for specimen SG·1 (Fig. 4).

Rhomb ⟨*a*⟩ *orientations*

The positive (r) and negative (z) rhomb pole figures for specimens SG·1 and SG·10 are completely separated (Fig. 3). These pole figures are strongly asymmetrical with respect to specimen fabric elements. Three distinct maxima are present in both the positive and negative rhomb pole figures for specimen SG·10, the dominant maximum in each pole figure being aligned within the *XZ* plane. Whilst the dominant r maximum is oriented perpendicular to the WNW plunging a-axis maximum, the dominant z maximum is perpendicular to the ESE plunging a-axis maximum (Fig. 3). In contrast, within specimen SG·1 none of the rhomb maxima are oriented perpendicular to the WNW plunging single a-axis maximum—a qualitative observation which could be interpreted (S.M. Schmid personal communication 1986) as indicating that the rhombs are not important slip planes in this tectonite. Two weakly populated r maxima symetrically inclined to the foliation pole (*Z*) within the *XZ* plane are recorded in specimen SG·1 (Fig. 3).

Study of the positive (r) and negative (z) rhomb poles

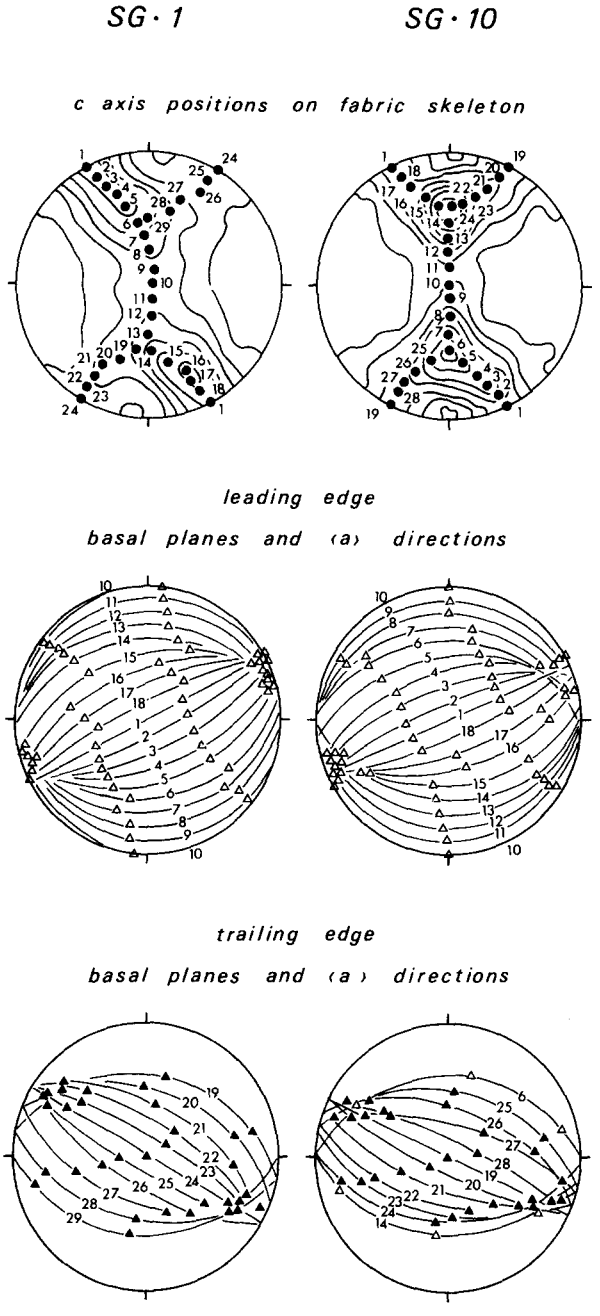

Fig. 4. Calculated positions of basal (0001) planes and ⟨a⟩ directions for different positions (numbered) on the c-axis fabric skeletons of specimens SG·1 and SG·10. Orientations of individual ⟨a⟩ directions lying within basal planes indicated by triangles. All lower hemisphere equal-area projections viewed towards the NNE. Note that only the 'leading edge' (ESE dipping girdle) of the c-axis fabric skeleton is characterized by c-axis positions (1–18) sharing a well defined common ⟨a⟩ direction.

corresponding to different positions on the c-axis fabric skeleton of specimen SG·10 indicates that distinct orientation fields exist for positive and negative rhomb poles (Fig. 5). This is most clearly illustrated in a traverse from positions 5 and 25 to position 9 where the r and z rhomb poles (Fig. 5) coincide with the rhomb pole maxima (Fig. 3). These c-axis positions on the central segment of the 'leading edge' are characterized by common WNW and ESE plunging ⟨a⟩ directions lying within positive (r) and negative (z) rhomb planes, respectively; poles to these rhomb planes are oriented close to the *XZ* plane (Fig. 5).

In contrast on the peripheral 'trailing edge' of the c-axis fabric skeleton (positions 13–27) poles to positive and negative rhombs define very different orientation fields (Fig. 5) which, in general, do not coincide with the rhomb pole figure maxima (Fig. 3). Consider first the positive (r) rhomb pole orientations for positions 13–27. One set of r poles forms a point concentration (Fig. 5) coincident with the point maximum lying within the *XZ* plane of the r pole figure (Fig. 3). The two other sets of r poles define an approximate small-circle distribution centred about this r point maximum with an opening angle of approximately 90°. The corresponding negative (z) poles for these c-axis positions define partial small-circles centred about the r point maximum with opening angles of 45 and 85° (Fig. 5). It is noteworthy that, with the exception of positions 13 and 14, the c-axes which define the peripheral 'trailing edge' of the fabric skeleton are perfectly aligned on a small-circle girdle of opening angle 48° centred about this r point maximum.

Thus the peripheral 'trailing edge' of the c-axis fabric skeleton for specimen SG·10 may be described as the rotation of a single crystal about that r rhomb pole which belongs to the point maximum lying within the *XZ* plane of the r pole figure. Traced around the peripheral 'trailing edge' of the fabric skeleton, ⟨a⟩ directions lying within this common r rhomb plane display a progressive change through 180° in orientation (Figs. 5 and 6).

Rhomb ⟨a⟩ orientations corresponding to different positions on the c-axis fabric skeleton have also been calculated for specimen SG·1 (Fig. 7). The rhomb ⟨a⟩ preferred orientation within this specimen is very similar to that described above for specimen SG·10, the 'leading' and peripheral 'trailing' edges of the fabric skeleton displaying totally different rhomb ⟨a⟩ preferred orientation characteristics (Fig. 7).

Two traverses have been made along the 'leading edge' of the c-axis fabric skeleton for specimen SG·1. In the first traverse, along the peripheral region of the 'leading edge', individual c-axis positions (6–1) are clearly related by rotation about a common WNW plunging ⟨a⟩ direction lying within one set of the positive (r) rhomb planes (left-hand diagram in middle row of Fig. 7). For the second traverse, along the central segment of the 'leading edge', individual c-axis positions (20 and 15–10) are related by WNW and ESE plunging ⟨a⟩ directions lying close to the *XZ* plane, within positive (r) and negative (z) rhomb planes, respectively (bottom row of Fig. 7). In contrast, c-axis positions (29–23) on the peripheral 'trailing edge' of the fabric skeleton are, as in specimen SG·10, related by a common WNW dipping positive (r) rhomb plane; ⟨a⟩ directions lying within this plane display a progressive change through 180° in orientation traced around the peripheral 'trailing edge' of the fabric skeleton (top row of Fig. 7).

The consistent orientation of one set of positive (r) rhomb planes on the peripheral 'trailing edge' of the c-axis fabric skeletons for specimens SG·10 and SG·1 suggests that this may be an important slip plane. However, the variable orientation of the ⟨a⟩ directions within this plane for different c-axis positions (e.g. specimen

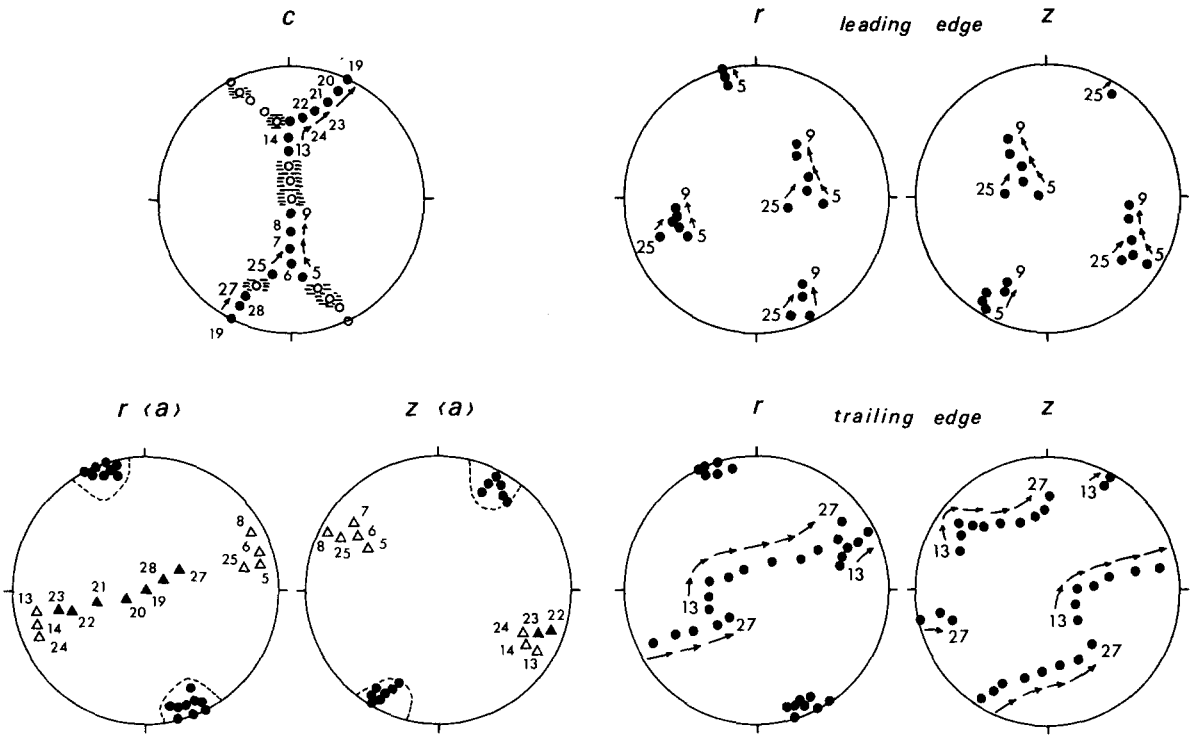

Fig. 5. Specimen SG·10. Calculated crystallographic preferred orientation associated with c-axis positions on the 'leading' (positions 1–18) and peripheral 'trailing' (positions 19–28) edges of the c-axis fabric skeleton. All lower hemisphere equal-area projections viewed towards the NNE. Note that the r and z poles (solid circles) on part of the 'leading edge' (positions 25, 5, 6, 7, 8, 9) are essentially related by WNW and ESE plunging common ⟨a⟩ directions (open triangles) lying within one set of positive (r) and negative (z) rhomb planes, respectively. In contrast, c-axis positions (13, 14 and 24, 23, 22, 21, 20, 19, 28, 27) on the peripheral 'trailing edge' of the fabric skeleton share a commonly oriented r rhomb plane; all the other r and z poles lie on small-circle girdles centred about this r pole maximum. Traced around the peripheral 'trailing edge' of the c-axis fabric skeleton, ⟨a⟩ directions lying within the common r rhomb plane display a progressive change through 180° in orientation (open triangles—⟨a⟩ directions for positions on central segment of c-axis fabric skeleton; closed triangles—⟨a⟩ directions for positions on peripheral 'trailing edge' of fabric skeleton). Orientations of z ⟨a⟩ rhomb systems whose poles coincide with the dominant z rhomb maxima in the *XZ* plane (Fig. 3) also indicated. Pecked lines on the r ⟨a⟩ and z ⟨a⟩ stereograms represent the corresponding 1.5 times uniform distribution contour (Fig. 3). Positions on c-axis fabric skeleton at which positive and negative forms are shown by the ODF to be interchangeable are indicated by open circles with horizontal bars.

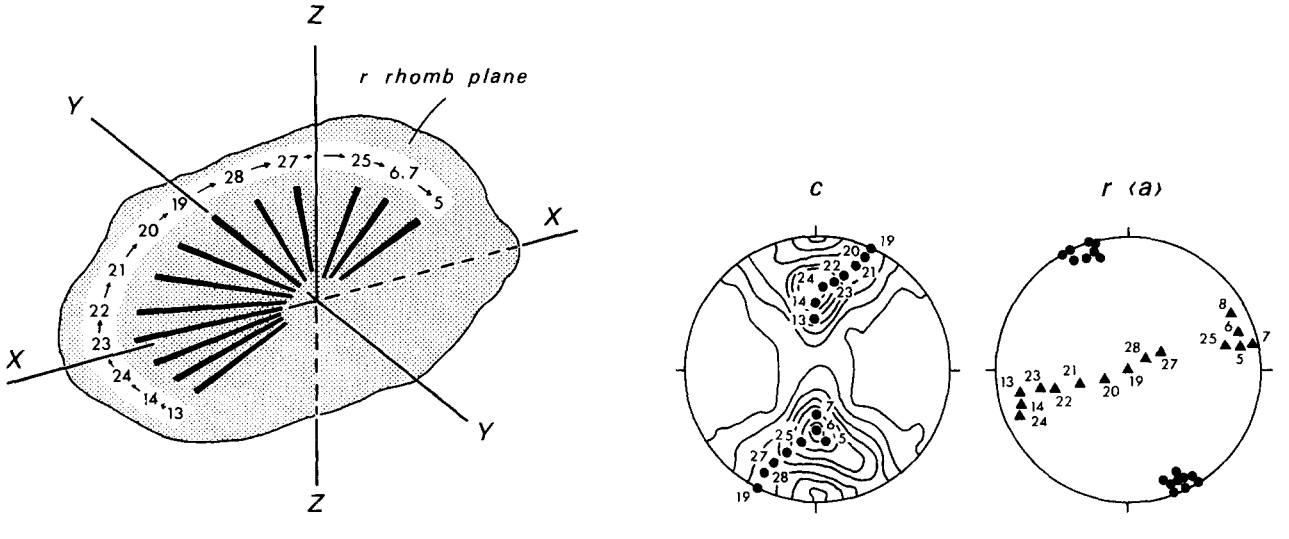

Fig. 6. Specimen SG·10. Relationships (for peripheral 'trailing edge' of c-axis fabric skeleton) between finite-strain axes ($X \geq Y \geq Z$), common rhomb plane and ⟨a⟩ directions (represented by radiating black lines) lying within this plane. Poles to common r rhomb planes and ⟨a⟩ directions lying within plane are represented (right stereogram) by solid circles and triangles, respectively. All lower hemisphere equal-area projections viewed towards the NNE.

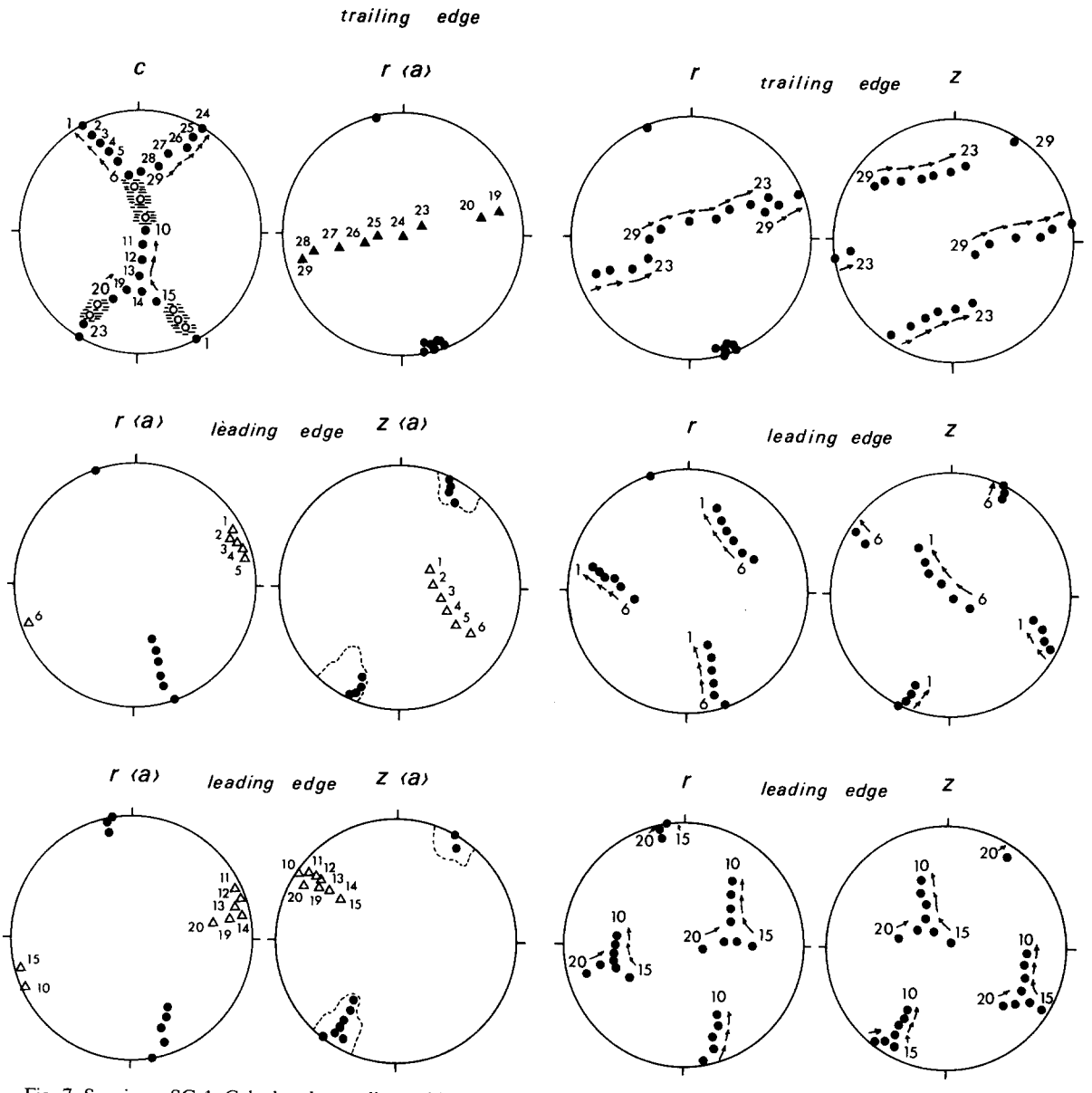

Fig. 7. Specimen SG·1. Calculated crystallographic preferred orientations associated with c-axis positions on the 'leading' (positions 1–18) and peripheral 'trailing' edges (positions 19–28) of the c-axis fabric skeleton. All lower hemisphere equal-area projections viewed towards the NNE. Poles to r and z rhomb planes—solid circles; ⟨a⟩ directions lying within the rhomb planes on the 'leading' and peripheral 'trailing' edges of the fabric skeleton—open and closed triangles, respectively. For the two traverses (middle and lower rows of stereograms) along the peripheral and central segments of the 'leading edge' of the fabric skeleton, different c-axis positions are related by either a common WNW plunging ⟨a⟩ direction (positions 6–1), or common WNW and ESE plunging ⟨a⟩ directions (positions 20, 15–10). In contrast on the peripheral 'trailing edge' of the fabric skeleton (top row) different c-axis positions are related by a commonly orientated r rhomb pole. Positions on the c-axis fabric skeleton at which positive and negative forms are shown by the ODF to be interchangeable are indicated by open circles with horizontal bars.

SG·10 in Fig. 6) suggests that either: (1) the crystallographic slip direction within the r slip plane varies with c-axis orientation or (2) that slip on the r plane is in the ⟨a⟩ direction, but that the geographical orientation of this crystallographic slip direction may vary from grain to grain.

Strong evidence for dominant crystallographic slip in the ⟨a⟩ direction has been recorded within quartz mylonites from many different tectonic environments (Schmid & Casey 1986) and therefore the former suggestion seems unlikely. The alternative interpretation of ⟨a⟩ slip varying in geographical orientation with c-axis position is most easily explained by deformation within the flattening field ($K \rightarrow 0$) of the strain plot.

INTERPRETATION OF 'INDIVIDUAL' CRYSTAL PREFERRED ORIENTATION

Preferred orientations of basal ⟨a⟩ and rhomb ⟨a⟩ systems on the 'leading edge' of the c-axis fabric skeleton for specimens SG·10 and SG·1 are very similar to those described within $L - S$ tectonites from other geological terrains (Schmid *et al.* 1981, Schmid & Casey 1986, Mancktelow 1987). These preferred orientation patterns (with basal, rhomb and prism planes containing a common ⟨a⟩ direction oriented within the XZ plane at a moderate angle to the lineation) are readily interpreted in terms of variable activity, for different c-axis positions, on the basal, rhomb and prism ⟨a⟩ slip systems

within a plane strain ($K = 1$) deformation regime (Bouchez & Pecher 1981, p. 47). However, as discussed above, detailed crystallographic preferred orientation on the peripheral 'trailing edge' of the fabric skeleton is most easily interpreted in terms of a flattening ($K \rightarrow 0$) deformation, with the dominant slip plane (r) remaining in a constant orientation but the inferred slip direction ⟨a⟩ variably oriented within this plane.

Thus it would appear that flow within specimens SG·10 and SG·1 (both $S > L$ tectonites) has, at the grain scale, been partitioned into domains of plane strain and flattening deformation, the resulting deformation, on the scale of the grain aggregate, keeping within the general flattening field of the strain plot ($1 > K > 0$). Whether these inferred domains consist of single or multiple grains is at present unknown; no obvious microstructural indications of their presence have been observed. Future A.V.A. studies are planned for characterizing both the size and distribution of these domains. Such an inferred (grain scale) partitioning of deformation has not previously been detected within naturally deformed quartzites; this may, however, reflect the general selection of $L - S$ (plane strain) tectonites for ODF analysis.

Implications for fabric simulations

Grain-scale deformation partitioning of the type detected within specimens SG·10 and SG·1 is not considered in the fabric simulations of Lister and co-workers (Lister *et al.* 1978, Lister & Paterson 1979, Lister & Hobbs 1980) which are based upon the fundamental assumption of a homogeneous strain field. This assumption requires that: (1) the shape change undergone by each grain is identical to that undergone by the aggregate as a whole; and (2) that five independent slip systems are activated (Full Constraints model) within each grain (see Lister *et al.* 1978, Van Houtte 1984 and Hobbs 1985 for discussion).

Within specimens SG·10 and SG·1 study of the complete crystallographic orientation corresponding to single c-axis positions indicates that individual 'grains' may have deformed along different strain paths from the bulk specimen. Similar examples of heterogeneous deformation have previously been detected by Van Houtte *et al.* (1984) and Wenk *et al.* (1986) within experimentally deformed calcite polycrystals. Fabric simulation models which permit such heterogeneous deformation have recently been reviewed by Van Houtte (1984) and Hobbs (1985). These models are characterized by a relaxation in the requirement of five independent slip systems within each grain (Relaxed Constraints models). Inverse pole figures predicted by such models for pure shear deformation were found by Van Houtte *et al.* (1984) to be very similar to those obtained from their axially symmetric flattening experiments (see also review by Wenk 1985, fig. 15). This observation has led Van Houtte *et al.* (1984) to suggest that individual grains in their experiments deform locally in plane strain and are arranged in such a way that the global shape fabric has an axial (oblate) symmetry. Similar crystallographic heterogeneities have been observed in metals and are called 'curling' to describe the bent grain shape microstructures produced by the necessity to maintain strain compatibility between neighbouring grains (Hosford 1964).

Implications for crystallographic fabrics as kinematic indicators

Within specimen SG·10 it is clearly the marked contrast between rhomb ⟨a⟩ preferred orientation on the 'leading' and peripheral 'trailing' edges of the c-axis fabric skeleton (Fig. 5) which has led to the major difference between the essentially symmetrical c-, a- and m-axis fabrics and the strongly asymmetrical fabrics for positive (r) and negative (z) rhombs (Fig. 3).

These results may have major implications for the general use of crystallographic fabric symmetry as a kinematic (strain path) indicator. As SG·10 is characterized by an oblate strain ellipsoid, flow within this specimen must have significantly departed from strict bulk simple shear. In terms of partitioning at the grain scale, grains belonging to the 'leading edge' population of the c-axis fabric could reflect deformation close to plane strain ($K = 1$) with a vorticity somewhere between pure and simple shear, whilst grains belonging to the peripheral 'trailing edge' population would reflect a contemporaneous, approximate flattening deformation ($K \rightarrow 0$), associated with a vorticity closer to coaxial flow. At the specimen scale deformation within this tectonite may be described as a non-coaxial flattening. Thus the symmetrical c, a and m pole figures in specimen SG·10 (Fig. 3), which were obtained by scanning over both types of inferred grain scale domain, are composite fabrics which do not reflect a homogeneous or strictly coaxial deformation.

Clearly the possibility of such heterogeneous grain scale deformation should be investigated within other tectonites whose symmetrical c- and a-axis fabrics have been used as evidence for coaxial flow. Within specimen SG·10 pole figure evidence for non-coaxial deformation is only provided by the asymmetrical r and z pole figures.

It should be emphasized, however, that asymmetrical rhomb pole figures should not be used in isolation as kinematic indicators. For example, it could be argued that the asymmetrical r and z pole figures in Fig. 3 have been produced by Dauphinée twinning acting upon an aggregate of grains whose r and z pole figures were originally symmetrical. This Dauphinée twinning could have ocurred either during or after the main intracrystalline deformation, and has previously been invoked by Baker & Wenk (1972) and Baker & Riekels (1977) to account for the difference in positive and negative crystallographic forms within quartz mylonites from the Stack of Glencoul area.

A Dauphinée twin is related to its host by a 180° rotation about the c-axis. In such twinning the crystal axes remain parallel, but the polarity of the a-axes is reversed; thus a positive trigonal form, such as r, is

exchanged for a negative form, such as z, and vica versa. For experimental axially symmetric flattening, Tullis & Tullis (1972) were able to demonstrate from inverse pole figure data that Dauphinée twinning resulted in a depletion of compression axes near the z rhomb poles and an augmenting of them near r. Thus, solely on the basis of the rhomb pole figure data for specimen SG·10 (Fig. 3) it could be argued (J. M. Christie personal communication 1986) that the asymmetry in the rhomb pole figures is due to Dauphinée twinning associated with uniaxial compression parallel to the positive (r) maximum in the pole figure.

The ODFs for specimens SG·10 and SG·1 indicate, however, that there is a strong interdependence of the preferred orientation of positive and negative forms with all other elements of the crystallographic fabric (Figs. 5 and 7). For example, whilst all crystal directions corresponding to c-axis positions on the 'trailing edge' of the fabric skeleton are related by rotation about a common r pole, crystal directions corresponding to c-axis positions on the 'leading edge' are related by rotation about a common ⟨a⟩ direction. Such relationships suggest (Schmid *et al.* 1981, p. 114) that, at least within each type of inferred grain scale domain, the crystallographic fabric has formed in response to a single and internally consistent mechanism of fabric formation rather than by the superimposition of fabric elements caused by glide with other elements caused by Dauphinée twinning.

DISCUSSION

Within the mylonitic quartzites at the Stack of Glencoul a clear relationship has been established between the pattern of quartz c- and a-axis fabrics within individual specimens and distance beneath the overlying Moine Thrust (Fig. 1, Tables 1 and 2). This relationship consists of a progressive spatial transition, with increasing finite strain and recrystallization, from symmetrical Type I cross-girdle c-axis fabrics (at 30 cm beneath the thrust) through asymmetrical cross-girdle fabrics to asymmetrical kinked single fabrics at 0.5 cm beneath the thrust surface. This c-axis fabric transition is accompanied by a concomitant change from essentially symmetrical two maxima a-axis fabrics through asymmetrical two maxima fabrics to asymmetrical dominantly single maxima a-axis fabrics.

Any model for this fabric transition at the Stack of Glencoul must take into account the following observations.

(1) Foliation within the entire mylonite sequence remains sub-parallel to the surface of the overlying Moine Thrust.

(2) Mylonites immediately adjacent to the thrust surface (specimens SG·1 and SG·2) are characterized by a dominant WNW plunging a-axis maximum which, although aligned within the XZ plane, is inclined at 24–27° to the lineation (Fig. 1, Table 1).

(3) The mylonites range from $S > L$ to $L - S$ tectonites. Measurement of the aspect ratios of relict grains within one of these specimens (SG·10) indicates that the grain shape fabric is approximately oblate with $K = 0.05$ (Schmid & Casey 1986, p. 270, specimen RL·8330). The calculated c-axis fabric for this specimen (Figs. 2 and 3) is transitional between a Type I cross-girdle and a small-circle girdle centred about the foliation pole (Z), suggesting (Schmid & Casey 1986, fig. 15) deformation intermediate between that of plane strain ($K = 1$) and flattening ($K = 0$). This strain symmetry interpretation is supported by the small-circle element of the a-axis fabrics within some of these mylonites (see Fig. 1, specimen SG·4; Fig. 3, specimen SG·10; and Law *et al.* 1986, fig. 6) which is also centred about Z.

(4) Different parts of the c-axis fabric skeleton are characterized by distinct 'single crystal' orientations (Figs. 5–7). On the ESE dipping 'leading edge' of the fabric skeleton individual c-axis positions are related by either: (i) a single common ⟨a⟩ direction oriented parallel to the WNW plunging a-axis maximum (peripheral region of 'leading edge' close to XZ plane) or (ii) two common ⟨a⟩ directions oriented parallel to the WNW and ESE plunging a-axis maxima (central region of fabric skeleton close to Y). In contrast, c-axis positions on the WNW dipping peripheral 'trailing edge' of the fabric skeleton are related by a common WNW dipping positive (r) rhomb plane; ⟨a⟩ directions lying within this common r plane progressively change through 180° in orientation traced around the peripheral 'trailing edge' of the fabric skeleton (Fig. 6).

(5) Such individual 'crystal' preferred orientation indicates that on the specimen scale deformation is heterogeneous. Grain scale domains of contemporaneous approximate plane strain and flattening deformation are inferred from this analysis and correspond to different positions on the 'leading' and 'trailing' edges of the c-axis fabric skeleton, respectively. The c- and a-axis fabrics in Fig. 1 (and Law *et al.* 1986, fig. 6) are therefore composite fabrics which do not reflect homogeneous deformation on the specimen scale.

Kinematic interpretation of crystallographic fabric transitions

Law *et al.* (1986) have argued that the gradual transition from symmetrical to asymmetrical c-axis fabrics at the Stack of Glencoul (Fig. 1) indicates the contemporaneous development of a vorticity gradient within the mylonites, ranging from strongly non-coaxial flow near the Moine Thrust to essentially coaxial flow at distances of greater than approximately 30 cm beneath the thrust. Such an interpretation is compatible with the a-axis fabrics in these tectonites (Fig. 1).

However, within specimen SG·10 the contrasting single crystal rhomb ⟨a⟩ preferred orientation on the 'leading' and 'trailing' edges of the symmetrical c-axis fabric has resulted in the formation of associated strongly asymmetrical positive (r) and negative (z) rhomb pole figures. Thus although the c, a and m pole figures for specimen SG·10 are symmetrical (Fig. 3) the total

crystallographic fabric within this tectonite is asymmetrical suggesting a non-coaxial deformation. Clearly the critical question to be asked is what is the degree of non-coaxiality (Means *et al.* 1980) associated with these asymmetrical total fabrics which contain symmetrical c-, a- and m-axis fabric elements? At present there are no reliable crystallographic fabric criteria for quantifying the degree of non-coaxiality associated with deformation (but see Platt & Behrmann 1986, p. 31).

The exact degree of non-coaxiality of deformation associated with mylonite formation therefore remains unknown. However, at the Stack of Glencoul, mylonites exhibiting symmetrical c- and a-axis fabrics are characterized by containing globular quartz grains whose c-axes are aligned sub-parallel to the shortening direction (Z); more flattened grains anastomose around these anomalous grains (Law *et al.* 1986, fig. 4). The preservation of these globular grains, which may locally be of detrital origin, has been taken by Law *et al.* (1986, p. 119) to indicate essentially coaxial strain paths. Such globular grains have not been observed within those mylonites located closer to the Moine Thrust which exhibit asymmetrical c- and a-axis fabrics.

In terms of deformation at the grain scale 'individual crystal' preferred orientation suggests that grains belonging to the 'leading edge' population of the c-axis fabrics could reflect deformation close to plane strain ($K = 1$) with a vorticity somewhere between pure and simple shear, whilst grains belonging to the peripheral 'trailing edge' population would reflect a contemporaneous flattening deformation ($K \rightarrow 0$) associated with a vorticity closer to coaxial flow.

Taking this interpretation further, the observed c- and a-axis fabric transition at the Stack of Glencoul (Fig. 1) could thus be viewed in terms of the increasing importance of the component of non-coaxial, plane strain deformation as the Moine Thrust is approached. Note, however, that even immediately adjacent to the Moine Thrust (specimen SG·1), the rhomb ⟨a⟩ preferred orientation (Fig. 7) indicates that flow has still significantly departed from bulk simple shear and involves a component of flattening deformation.

It is proposed that flow within the mylonites at the Stack of Glencoul can be represented by a single value of approximately coaxial flattening ($K \rightarrow 0$) and a marked gradient of non-coaxial plane strain deformation which increases towards the Moine Thrust. The degree of non-coaxiality of the plane strain component is unknown. However, a feature of plane strain simple-shear deformation is that strain compatibility can be maintained in the presence of a strain gradient; this is not the case with plane strain pure shear deformation. Detailed examples of such strain compatibility considerations within thrust sheets are given by Sanderson (1982) and Law & Potts (1987). Therefore it is considered that flow within the Stack of Glencoul mylonites can be represented by a single value of flattening deformation and a marked gradient of simple shear which increases towards the thrust. The total deformation may be described as non-coaxial flattening.

This interpretation is compatible with the observation that although the intensity of deformation within these $S > L$ tectonites increases towards the Moine Thrust, the mylonitic foliation, irrespective of distance beneath the thrust, is parallel to it. Such observations cannot be accounted for in a model invoking a gradient of simple shear deformation alone. A similar form of strain factorization to that described above has previously been proposed for the Stack of Glencoul mylonites by Sanderson (1982, p. 215) who, on the basis of then available strain data, suggested that mylonite formation may have involved components of both pure and simple shear deformation.

Significance of dominant a-axis maximum

On the basis of strain compatibility arguments it has been suggested above that grains belonging to the 'leading edge' of the c-axis fabric skeleton must be reflecting the plane strain simple shear component of the bulk deformation within these tectonites. Study of 'individual crystal' orientations within specimens SG·1 and SG·10 (Figs. 5 and 7) indicates that it is grains corresponding to these c-axis positions which are responsible for the WNW plunging a-axis maximum in the composite a-axis fabrics (Figs. 1 and 3). These a-axis maxima although aligned within the XZ plane, are inclined at 29–17° to both the lineation and the overlying foliation parallel to the Moine Thrust plane (Tables 1 and 2).

Following the simulation work of Etchecopar (1977) it has been proposed (e.g. Burg & Laurent 1978, Bouchez 1978, Bouchez *et al.* 1979) that in simple shear deformation, the dominant crystallographic slip direction ⟨a⟩ within individual grains will tend to become aligned parallel to the direction of bulk simple shear deformation (Burg & Laurent 1978, fig. 14). If this model is applicable to the plane strain deformation domains within the Stack of Glencoul mylonites then, assuming that the Moine Thrust represents the orientation of the bulk simple shear plane, one would expect the dominant ⟨a⟩ maxima associated with these domains to be aligned parallel to both the lineation and the overlying thrust plane. This is clearly not the case (Fig. 1).

Similar anomalous relationships between lineation and the dominant a-axis maximum have been described from other mylonite zones (Boullier & Quenerdel 1981, Mancktelow 1987) and, in general these could be due to: (1) the simultaneous operation of two slip systems; (2) a departure from bulk simple shear conditions; or (3) a complex deformation history.

Many $L - S$ tectonites display Type I cross-girdle c-axis fabrics having a paired arrangement of favoured slip planes which intersect in Y, with the slip directions ⟨a⟩ arranged to either side of the foliation (e.g. Schmid & Casey 1986, fig. 11). Over a volume involving many grains this effectively gives the aggregate two independent shear systems which is sufficient for homogeneous plane strain in the XZ plane. Mancktelow (1987) has shown that within mylonites exhibiting cross-girdle c-axis fabrics the anomalously large angle between linea-

tion and the dominant a-axis maximum may be due to the operation of paired intracrystalline shear systems which straddle both the foliation and the bulk shear flow plane. As pointed out by Mancktelow the sense of shear in both sets must be the same (i.e. they are not a conjugate set) in order that the bulk shear direction remains one of no longitudinal strain. In this model it is the c-axis orientation of individual grains that determines which of the two shear systems a particular grain uses. Such a model, which incorporates plane strain deformation for grains on both the 'leading' and 'trailing' edges of the cross-girdle c-axis fabric, cannot be applicable to the Stack of Glencoul mylonites. Within these $S > L$ tectonites it has been demonstrated above that grains belonging to the 'leading' and 'trailing' edges of the c-axis fabric skeleton are characterized by 'individual crystal' orientations indicative of plane strain and flattening deformation, respectively. Thus if two shear systems are operating simultaneously to produce the anomalous relationship between lineation and the dominant a-axis maximum, they must both be operating within individual grains (duplex slip) on the 'leading edge' of the fabric skeleton.

Alternatively it could be argued that the anomalously large angle between lineation and dominant a-axis maximum within these $S > L$ tectonites is due to the flattening component of deformation. However, on the basis of 'individual crystal' orientations and strain compatibility considerations it has been suggested above that grains on the 'leading edge' of the fabric skeleton are characterized by plane strain, simple shear deformation. The possible effect of deformation within the inferred flattening domains remains unclear.

It could also be argued that the last increments of deformation have been coaxially imposed, increasing the angle between the dominant a-axis maximum and the lineation, but leaving the a-axis maxima unmodified in terms of relative intensity. A similar general fabric overprinting model has previously been proposed by Bouchez *et al.* (1983, p. 415). However, as will be argued below, such an overprinting would surely reset the rhomb ⟨a⟩ preferred orientation on both the leading and trailing edges of the fabric skeleton.

Thus it must be concluded that the large angle between lineation and the dominant a-axis maximum remains an enigma which cannot easily be reconciled with the other deformation features in these tectonites.

Relative ages of plane strain and flattening components

Christie (1963, p. 405) has interpreted symmetrical c-axis fabrics from the Stack of Glencoul as indicating a late (post-thrusting) coaxial flattening superimposed upon originally asymmetrical fabrics produced by shearing deformation. In this interpretation all mylonites, irrespective of distance beneath the Moine Thrust, were considered to have originally been characterized by asymmetrical c-axis fabrics. However, with the discovery of the c- and a-axis fabric transition at the Stack of Glencoul (Fig. 1), it became clear that formation of the asymmetrical c- and a-axis fabrics near the thrust surface (non-coaxial flow associated with WNW directed overthrusting) must either be contemporaneous with, or later than, formation of the essentially symmetrical fabrics at greater distances beneath the thrust (Law *et al.* 1986). If the overprinting model of Christie (1963) were correct then: (1) the asymmetrical fabrics close to the thrust surface would be overprinted by symmetrical fabrics; and (2) symmetrical fabrics would be detected within the most highly deformed rocks. These predictions are clearly not compatible with the observed crystallographic fabric transition and associated microstructures.

Detailed study of 'individual crystal' orientations on the 'leading' and 'trailing' edges of the c-axis fabric skeleton within specimens SG·1 and SG·10 (0.5 cm and 4.6 m beneath the thrust, respectively) allows a further refinement on interpreting the relative ages of the components of flattening and shearing deformation. As both tectonites are characterized by 'single crystal' preferred orientations indicative of plane strain and flattening deformation on the 'leading' and 'trailing' edges, respectively, of the c-axis fabric skeleton (Figs. 5–7) it is considered that these strain components must be contemporaneous. If the plane strain (shearing) component had been superimposed upon the flattening component (or vica versa) this would surely have reset the 'single crystal' preferred orientations on both the 'leading' and 'trailing' edges of the fabric skeleton.

Acknowledgements—X-ray texture goniometry was carried out at ETH, Zurich, Switzerland. This study, which was supported by NERC research grant GR3/4612, would not have been possible without the constant help and encouragement of Martin Casey and Stefan Schmid who also provided the basic ODF data for specimens SG·1 and SG·10. Jean-Luc Bouchez, John Christie and Stefan Schmid are thanked for their critical reviews of an earlier version of the manuscript.

REFERENCES

Baker, D. W. & Wenk, H. R. 1972. Preferred orientation in a low symmetry mylonite. *J. Geol.* **80**, 81–105.

Baker, D. W. & Riekels, L. M. 1977. Dauphinée twinning in quartzite mylonite. *J. Geol.* **85**, 15–26.

Behrmann, J. H. & Platt, J. P. 1982. Sense of nappe emplacement from quartz c-axis fabrics: an example from the Betic Cordilleras (Spain). *Earth Planet. Sci. Lett.* **59**, 208–215.

Bouchez, J.-L. 1978. Preferred orientations of quartz a-axes in some tectonites: kinematic inferences. *Tectonophysics* **49**, T25–T30.

Bouchez, J.-L., Dervin, P., Mardon, J. P. & Englander, M. 1979. La diffraction neutronique appliquée à l'étude de l'orientation préférentielle de réseau dans les quartzite. *Bull. Mineral.* **102**, 255–231.

Bouchez, J.-L., Lister, G. S. & Nicolas, A. 1983. Fabric asymmetry and shear sense in movement zones. *Geol. Rdsch.* **72**, 401–419.

Bouchez, J.-L. & Pecher, A. 1981. The Himalayan Main Central Thrust Pile and its quartz-rich tectonites in Central Nepal. *Tectonophysics* **78**, 23–50.

Boullier, A.-M. & Quenardel, J.-M. 1981. The Caledonides of northern Norway: relation between preferred orientation of quartz lattice, strain and translation of the nappes. In: *Thrust and Nappe Tectonics* (edited by McClay, K. R. & Price, N. J.). *Spec. Publs Geol. Soc. Lond.* **9**, 185–195.

Burg, J. P. & Laurent, P. 1978. Strain analysis of a shear zone in a granodiorite. *Tectonophysics* **47**, 15–42.

Christie, J. M. 1963. The Moine thrust zone in the Assynt Region, northwest Scotland. *Univ. Calif. Publs geol. Sci.* **40**, 345–440.

Etchecopar, A. 1977. A plane kinematic model of progressive deformation in a polycrystalline aggregate. *Tectonophysics* **39**, 121–139.

Hobbs, B. E. 1985. The geological significance of microfabric analysis. In: *Preferred Orientations in Deformed Metals and Rocks* (edited by Wenk, H.-R.). Academic Press, New York, 463–484.

Hosford, W. F. 1964. Microstructural changes during deformation of [011] fiber-textured metals. *Trans. Metal. Soc. AIME* **230**, 12–15.

Law, R. D. 1986. Relationships between strain and quartz crystallographic fabrics in the Roche Maurice quartzites of Plougastel, western Brittany. *J. Struct. Geol.* **8**, 493–516.

Law, R. D., Casey, M. & Knipe, R. J. 1986. Kinematic and tectonic significance of microstructures and crystallographic fabrics within quartz mylonites from the Assynt and Eriboll regions of the Moine Thrust zone, NW Scotland. *Trans. R. Soc. Edinb., Earth Sci.* **77**, 99–126.

Law, R. D., Knipe, R. J. & Dayan, H. 1984. Strain path partitioning within thrust sheets: microstructural and petrofabric evidence from the Moine Thrust zone at Loch Eriboll, northwest Scotland. *J. Struct. Geol.* **6**, 477–497.

Law, R. D. & Potts, G. J. 1987. The Tarskavaig Nappe of Skye, northwest Scotland: a re-examination of the fabrics and their kinematic significance. *Geol. Mag.* **124**.

Lister, G. S. 1977. Crossed-girdle c-axis fabrics in quartzites plastically deformed by plane strain and progressive simple shear. *Tectonophysics* **39**, 51–54.

Lister, G. S. & Hobbs, B. E. 1980. The simulation of fabric development during plastic deformation and its application to quartzite: the influence of deformation history. *J. Struct. Geol.* **2**, 355–370.

Lister, G. S. & Patterson, M. S. 1979. The simulation of fabric development during plastic deformation and its application to quartzites: fabric transitions. *J. Struct. Geol.* **1**, 99–116.

Lister, G. S., Patterson, M. S. & Hobbs, B. E. 1978. The simulation of fabric development in plastic deformation and its application to quartzite: the model. *Tectonophysics* **45**, 107–158.

Lister, G. S. & Snoke, A. 1984. S-C mylonites. *J. Struct. Geol.* **6**, 617–638.

Lister, G. S. & Williams, P. F. 1979. Fabric development in shear zones, theoretical controls and observed phenomena. *J. Struct. Geol.* **1**, 283–297.

Lister, G. S. & Williams, P. F. 1983. The partitioning of deformation in flowing rock masses. *Tectonophysics* **92**, 1–33.

Mancktelow, N. S. 1987. Quartz textures from the Simplon Fault Zone, SW Switzerland and N. Italy. *Tectonophysics*. In press.

Marjoribanks, R. W. 1976. The relation between microfabric and strain in a progressively deformed quartzite sequence from Central Australia. *Tectonophysics* **32**, 269–293.

Means, W. D., Hobbs, B. E., Lister, G. S. & Williams, P. F. 1980. Vorticity and non-coaxiality in progressive deformations. *J. Struct. Geol.* **2**, 371–378.

Platt, J. P. & Behrmann, J. H. 1986. Structures and fabrics in a crustal scale shear zone, Betic Cordilleras, SE Spain. *J. Struct. Geol.* **8**, 15–34.

Price, G. P. 1985. Preferred orientations in quartzites. In: *Preferred Orientations in Deformed Metals and Rocks* (edited by Wenk, H.-R.). Academic Press, New York, 385–406.

Reikels, L. M. & Baker, D. W. 1977. The origin of the double maximum of optic axes in quartzite mylonites. *J. Geol.* **85**, 1–14.

Sanderson, D. J. 1982. Models of strain variation in nappes and thrust sheets: a review. *Tectonophysics* **88**, 201–233.

Schmid, S. M. & Casey, M. 1986. Complete fabric analysis of some commonly observed quartz c-axis patterns. In: *Mineral and Rock Deformation: Laboratory Studies—The Paterson Volume* (edited by Hobbs, B. E. & Heard, H. C.). *Am. geophys. Union, Geophys. Monogr.* **36**, 263–286.

Schmid, S. M., Casey, M. & Starkey, J. 1981. An illustration of the advantages of a complete texture analysis described by the Orientation Distribution Function (ODF) using quartz pole figure data. *Tectonophysics* **78**, 101–117.

Simpson, C. & Schmid, S. M. 1983. An evaluation of criteria to deduce the sense of movement in sheared rocks. *Bull. geol. Soc. Am.* **94**, 1281–1288.

Starkey, J. 1970. A computer program to prepare orientation diagrams. In: *Experimental and Natural Rock Deformation* (edited by Paulitsch, P.). Springer Verlag, Berlin, 51–74.

Tullis, J. & Tullis, T. E. 1972. Preferred orientation produced by mechanical Dauphinée twinning: thermodynamics and axial experiments. In: *Flow and Fracture of Rocks* (edited by Heard, H., Borg, I., Carter, N. & Raleigh, C.). *Am. geophys. Union, Geophys. Monogr.* **16**, 67–82.

Van Houtte, P. 1984. Some recent developments in the theories for deformation texture prediction. In *Proceedings 7th International Conference on Textures of Materials* (edited by Brakman, C. M., Jongenburger, P. & Mittemeijer, E. J.). *Netherlands Soc. Mat. Sci., Zwijndrecht*, 7–23.

Van Houtte, P., Wenk, H. R. & Wagner, F. 1984. The curling effect as a possible explanation of the uniaxial compression textures of calcite. In: *Proceedings 7th International Conference on Textures of Materials* (edited by Brakman, P., Jongenburger, P. & Mittemeijer, E. J.). *Netherlands Soc. Mat. Sci., Zwijndrecht*, 153–158.

Wenk, H.-R. 1985. Carbonates. In: *Preferred Orientations in Deformed Metals and Rocks* (edited by Wenk, H.-R.). Academic Press, New York, 361–384.

Wenk, H.-R., Kern, H., Van Houtte, P. & Wagner, F. 1986. Heterogeneous deformation in axially deformed calcite polycrystals. In: *Mineral and Rock Deformation: Laboratory Studies—The Paterson Volume* (edited by Hobbs, B. E. & Heard, H. C.). *Am. geophys. Union, Geophys. Monogr.* **36**, 287–295.